

Chapter 2

Airborne and Space-borne Remote Sensing of Cryosphere

Kenneth C. Jezek

Glossary

Cryosphere	Those components of the Earth system that contain water in its frozen form.
Radar	Radio detection and ranging systems.
Lidar	Light detection and ranging systems.
Radiometers	Radio frequency receivers designed to detect emitted radiation from a surface and in accordance with Planck's law.
Synthetic aperture radar	Radar system which increases along track resolution by using the motion of the platform to synthesize a large antenna.
Permafrost	Persistently frozen ground.
Ice sheet	Continental-scale, freshwater ice cover that deforms under its own weight.
Sea ice	Saline ice formed when ocean water freezes.
Glaciers	Long, channelized, slabs of freshwater ice thick enough to deform under their own weight.
Seasonal snow	The annual snow that blankets land cover in the winter and melts by summer.

This chapter was originally published as part of the Encyclopedia of Sustainability Science and Technology edited by Robert A. Meyers. DOI:[10.1007/978-1-4419-0851-3](https://doi.org/10.1007/978-1-4419-0851-3)

K.C. Jezek (✉)

Byrd Polar Research Center, School of Earth Sciences, The Ohio State University,
1090, Carmack Road, Columbus, OH, USA

e-mail: jezek.1@osu.edu

Definition of the Subject: The Cryosphere

The Cryosphere broadly constitutes all the components of the Earth system which contain water in a frozen state [1]. As such, glaciers, ice sheets, snow cover, lake and river ice, and permafrost make up the terrestrial elements of the Cryosphere. Sea ice in all of its forms, frozen sea bed and icebergs constitute the oceanic elements of the Cryosphere while ice particles in the upper atmosphere and icy precipitation near the surface are the representative members of the Cryosphere in atmospheric systems. This overarching definition of Earth's cryosphere immediately implies that substantial portions of Earth's land and ocean surfaces are directly subject in some fashion to cryospheric processes. Through globally interacting processes such as the inevitable transfer of heat from the warm equatorial oceans to the cold polar latitudes, it seems reasonable to argue that all regions of Earth are influenced by cryospheric processes and their integration into the modern climate of the planet. Observations of the cryosphere necessary to predict future variability in Earth's ice cover and its interaction with other Earth systems must be made on commensurate spatial and temporal scales. Consequently, airborne and space-borne remote sensing technologies with global reach play a key role in acquiring data necessary to understand the important physical processes and earth system interactions that govern the evolution of the Cryosphere (Fig. 2.1).

Introduction

The broad spatial and seasonally changing distribution of ice plays an important role in earth systems and human activities. At high latitudes, ice covered land and ocean surfaces are highly reflective thus redirecting incoming solar radiation back into space in the summer months. Indeed, reductions in the spatial area of snow and ice cover are believed to be an important feedback mechanism that enhances warming at high latitudes [2, 3]. Essentially, reduced snow and ice cover exposes darker land and ocean surfaces that retain rather than reflect solar energy. This results in increased warming and hence a further decrease in the area of snow and ice covered surfaces. Sea ice is an important habitat for birds such as penguins and mammals such as seals and polar bears which thrive in this icy environment [4]. But the underside of sea ice is also an important refuge for some of the smallest creatures including the shrimp-like krill which graze upon algae that grows just beneath and within the ice canopy [5, 6]. Terrestrial permafrost and frozen sediments beneath the oceans support an important reservoir of organic carbon and gas hydrates [7]. As permafrost melts, methane can be released contributing to the increasing concentration of greenhouse gases in the atmosphere. Glaciers and ice sheets are vast reservoirs of Earth's freshwater. As the ice sheets thin, water flows from the ice sheets into the oceans raising global sea level [8]. In terms of our daily activities, seasonal snow and glaciers are important sources of spring runoff

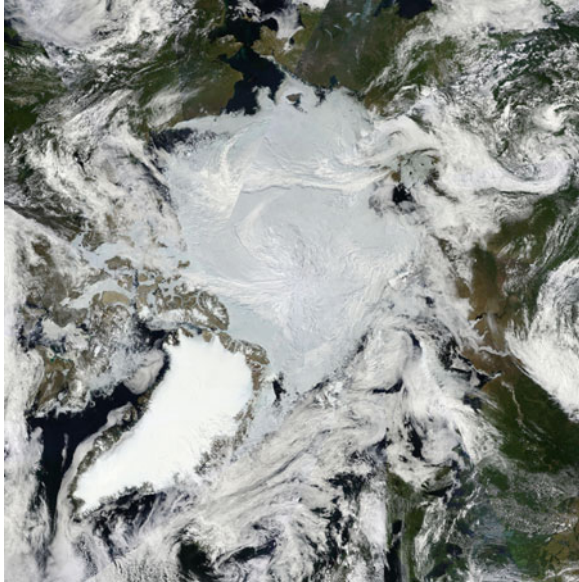


Fig. 2.1 NASA MODIS composite for July 7, 2010. Starting in the *lower left* quadrant and going clockwise, the Greenland sheet is almost cloud free as are the adjacent smaller ice caps on the Canadian Arctic Islands. Much of northern Canada and Alaska are cloud covered till the Bering Strait which is also almost sea ice free. Patches of sea ice cling to the Asian coast and there is a smattering of snow cover on the Putorana Mountains in western Siberia. The Gulf of Ob, Novaya Zemlya, the Franz Josef Land, and Spitsbergen Islands are barely visible through the cloud. The central Arctic basin is covered by sea ice. The image illustrates the scale of the cryosphere as well as some of the complications faced when trying to study it from space (Image prepared by NASA's MODIS Rapid Response team)

for irrigation and power generation, while ice jams on rivers constitute important obstacles to winter-time navigation and can cause low-land flooding [9]. Thawing permafrost causes the land near surface to become unstable which can result in catastrophic structural failures in buildings.

The global span of cryospheric processes and the strong daily to seasonal swing in the extent of snow and ice makes studying and monitoring the cryosphere an especially challenging scientific objective [10]. Moreover the variety of forms in which ice can be manifest in Earth systems means that no single observing system is capable of making adequate observations. Rather an ensemble of techniques is required to fully appreciate and eventually understand the complexities of the cryosphere and its interaction with other earth systems. Locally, observing tools may include direct, field measurements of snow pack thickness or physical temperature. Much different sets of tools are needed to characterize the cryosphere on a global and annual scale where the inhospitable climate and the physical remoteness of many sectors of the cryosphere represent obstacles to scientific investigation. Here, aircraft and spacecraft mounted instruments are required to infer geophysical properties from a remote distance (Fig. 2.2).

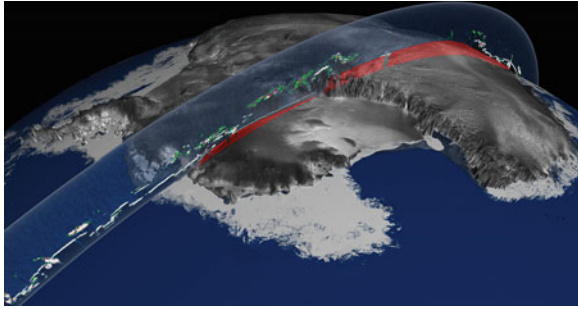


Fig. 2.2 Illustration of NASA's ICESat passing over the Antarctic. ICESat collected repeat elevation data over ice sheets and sea ice to study changing ice thicknesses. ICESat also sounded the atmosphere to study aerosols. NASA/Goddard Space Flight Center Scientific Visualization Studio, RADARSAT mosaic of Antarctica (Canadian Space Agency)

Compounded with these geographic challenges, observations of the icy surface often have to overcome cloud cover that frequently obscures the high latitudes, as well as continuing measurements during the long polar night. Consequently a range of instruments generally rely on distinguishing properties evident in the broad-spectral electrical characteristic of icy terrain. For example, even the cloudy atmosphere is largely transparent to microwave radiation. That fact combined with the very different microwave emission of open ocean and sea ice enables space-borne microwave observations of annual sea ice extent and concentration day and night and in all weather. Similarly the electrical contrast between rock and ice enables airborne radio frequency radar measurements of the thickness of polar ice sheets and glaciers. However some of the most recent advances in cryospheric science have been made by relying on one of the most basic properties of the icy cover, namely its mass. Space-borne measurements of the changing gravitational attraction of variably sized snow and ice bodies enables direct estimates of changing polar ice mass and the redistribution of melting ice into the liquid oceans. Indeed it can be argued that engineering and technological advances in airborne and remote sensing have had some of their greatest scientific impacts in the understanding the evolution of Earth's ice cover.

This article provides an overview of remote sensing of the cryosphere from both aircraft and spacecraft. A brief historical review of remote sensing of snow and ice is followed by a discussion of the physics of remote sensing of the cryosphere and how developments in remote sensing have led to a series of important scientific advances. These include the realization of the diminishing extent of Arctic sea ice and the thinning of glaciers, ice caps, and ice sheets worldwide. Both of these observations form critical, direct evidence of changing world climate. The article concludes with a discussion of developing international collaborations that are aimed at pooling technologically sophisticated and operationally expensive international assets so as to obtain an integrated system of continuing remote sensing observations necessary to predict future changes in Earth's ice and the consequent impacts on human activities.

Early History of Cryospheric Remote Sensing

The science and operational communities have always been quick to adopt new instruments and platforms for use in observing snow and ice in all of its forms. This section reviews early developments in cryospheric remote sensing – which were in part driven by science and in part by the basic desire to explore the most remote regions of Earth.

Airborne Photo-Reconnaissance

Aerial photography of ice covered terrain began during early twentieth century expeditions to the high altitudes and was used primarily to document the progress of the expedition. Survey quality aerial mapping was adopted using techniques primarily developed during World War I [11]. Mittelholzer and others [12] writing about the 1923 Junkers Expedition to Spitzbergen offer a very complete overview of the geographic and cartographic objectives for aerial photography in the North including a brief discussion of glacier formation as revealed by the aerial photographs. They also give an interesting technical discussion of the challenges faced when doing aerial photographic reconnaissance over highly reflective snow-covered terrain.

Wilkins documented ice cover in the Antarctic Peninsula during the first successful flight in Antarctica by using a hand-held, folding Kodak 3A camera [13, 14]. Richard E. Byrd devoted time and resources to aerial photography for quantitative surveying purposes during his first Antarctic Expedition of 1928–1930. In his book, “Little America,” Byrd [15] writes that photographs from Ashley McKinley’s laboratory provided “perhaps, the most important geographical information from the expedition.” McKinley was third in command of the expedition and the aerial surveyor. McKinley operated his Fairchild K-3 mapping camera during Byrd’s 1929 historic flight to the South Pole.

These early airborne photographic records were acquired with great skill and at considerable risk. The quality of the photographs is often exceptional and the photos themselves represent an oft under-utilized resource for directly gauging century-scale changes in Earth’s ice cover.

Satellite Photography

A mere 32 years after Byrd’s aerial photographic surveying in Antarctica, space-borne cameras began capturing unique pictures of Earth. CORONA, ARGON, and LANYARD were the first three operational imaging satellite reconnaissance systems and they acquired data during the early 1960s for both detailed reconnaissance purposes and for regional mapping [16–18]. Early reconnaissance satellite

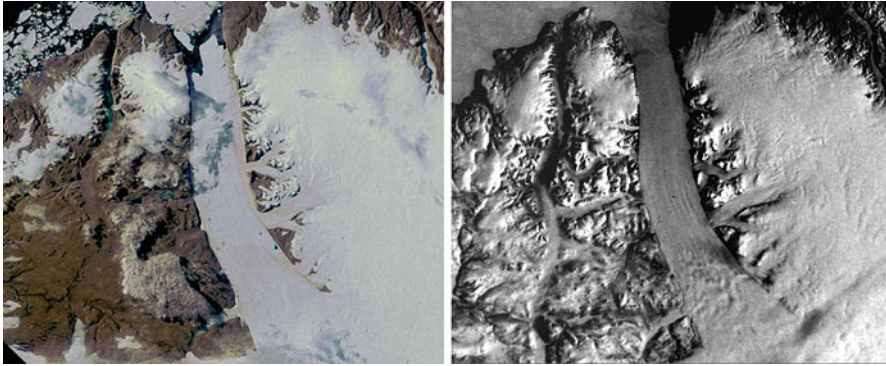


Fig. 2.3 European Space Agency MERIS image of Peterman Glacier, Greenland (*left*). The multispectral image was acquired in July, 2008 and before a large part of the floating ice tongue broke free. Argon panchromatic photograph acquired during the spring of 1962. The clarity of this early view from space is exceptional and provides a valuable gauge for assessing changes in glacier ice from the 1960s to the present

photographs provide a unique view of our world as it appeared at the beginning of the space age. Researchers in the environmental science community are the most recent beneficiaries of these data after they were declassified and made publicly available in 1995 through the efforts of Vice President Al Gore along with several government agencies working together with civilian scientists as part of the MEDEA program [19]. Polar researchers in particular inherited a wealth of detailed photography covering both of the great polar ice sheets. After processing with sophisticated digitizing instruments and subsequent analysis with modern photogrammetric and image processing techniques, investigators have shown that these data can be used to characterize local fluctuations in glacier termini [20, 21], investigate large-scale flow features on ice sheets [22, 23] and to measure long-term average velocity by feature retracking techniques [24] (Fig. 2.3).

Development of Depth Sounding Radar

Early suggestions that glaciers were penetrated by radio signals are attributed to observations made at Little America during Byrd's 2nd Antarctic Expedition [25]. This observation, along with reports that pulsed radar altimeters were yielding faulty readings over glaciers, led to the first radar experiments to measure ice thickness in 1955. In 1960, Waite and Schmidt [25] made measurements over Greenland from aircraft at 110, 220, 440, and 4,300 MHz. These results initiated a revolution in glaciology because the ice thickness and internal structure of glaciers and ice sheets could be rapidly sounded from aircraft [26].

Although the sophistication of ice sounding radar systems has increased tremendously, the basic principle of the technique remains the same and continues

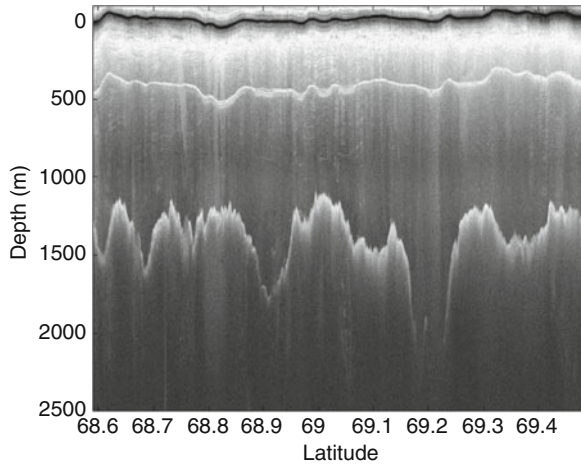


Fig. 2.4 North south airborne profile of ice thickness in west central Greenland. The *upper black line* is the radar reflection from the snow surface. The line at about 500 m depth is a multiple echo of the surface from the aircraft itself. The undulating line at an average depth of about 1,400 m is the reflection from the glacier bottom. The profile crosses the upstream segment of Jakobshavn Glacier at 69.2° N 48.1°W. There the 2,000 m thick ice has incised a deep channel into the bedrock. The data were acquired by the University of Kansas in 2008

to be a fundamental tool used by researchers (Fig. 2.4). Essentially, the one-way travel time of a radar pulse transmitted through the ice or snow is multiplied by the appropriate wave speed and the thickness so determined. More complex, two dimensional maps of the glacier bed topography can be assembled from multiple profiles that are combined using travel time migration techniques [27]. Several snow and ice sounding radars are part of the primary instrument suite presently carried aboard aircraft supporting NASA's IceBridge program [28].

Depth sounding radar remains one of the few techniques available to researchers interested in probing the volume of the terrestrial ice cover and the properties of the underlying bed. Airborne radars have been successfully used to study glacier, ice sheets, and to a more limited degree sea ice and permafrost. Seismic techniques yield important complementary information but can be carried out only in situ. Airborne gravity measurements provide important regional information but are generally less accurate than the radar technique for measurements on glaciers.

Scientific Advances from Airborne and Space-borne Remote Sensing

In most instances, airborne and space-borne platforms carry similar kinds of remote sensing instruments. Often times, space-borne instruments are first proto-typed as part of initial airborne campaigns. However, advantages of instrument installations

on multiple kinds of platforms go far beyond vetting the effectiveness of an instrument. For example, space-borne systems can provide global scale observations, with some imaging instruments yielding pole-to-pole observations on a daily basis. Manned and increasingly unmanned aircraft, with their ability to maneuver and loiter over an area, can provide much denser spatial and temporal coverage when profiling instruments, such as altimeters, are of interest. This section begins with a review of remote sensing physics and then summarizes key applications of remote sensing to several cold regions themes.

Basics of Remote Sensing of the Cryosphere

Airborne and space-borne sensors measure local changes in electromagnetic, gravitational, and magnetic force fields. Disturbances can arise from the passive, thermodynamically driven electromagnetic radiation emitted by the earth's distant surface, or the reflectance of incoming solar radiation from the Earth's surface, both of which change with the terrain type. Instruments and associated satellites of this type include the Electrically Scanning Microwave Radiometer (ESMR), Scanning Multichannel Microwave Radiometer (SMMR), Special Sensor Microwave Radiometer (SSM/I), Advanced Very High Resolution Radiometer (AVHRR), Landsat, Moderate Resolution Imaging Spectrometer (MODIS), Medium Resolution Imaging Spectrometer (MERIS), Satellite Pour l'Observation de la Terre (SPOT). Disturbances can also arise from the active behavior of the sensor itself. Radars and lidars include the Airborne Topographic Mapper (ATM), Laser Vegetation Imaging Sensor (LVIS), synthetic aperture radar (SAR) and radar altimeters on the European Remote Sensing Satellite (ERS-1/2), RADARSAT 1/2, synthetic aperture radar and radar altimeter on Envisat, Phased Array L-band SAR, TerraSAR-X, GEOSAT, the Ice and Climate Experiment Satellite (ICESat) lidar, the Cryosat radar altimeter. These instruments illuminate the surface with electromagnetic signals, which upon reflection can be detected back at the sensor after an elapsed time. Local changes in the gravity field at airborne and space-borne elevations are indications of changes in the distribution of mass within the Earth. Such instruments include airborne gravimeters on NASA's IceBridge, NASA's Gravity Recovery and Climate Experiment (GRACE) satellite, and ESA's Gravity field and Ocean Circulation Explorer (GOCE) satellite.

The task of the remote sensing scientist is to take measurements of these basic force fields and infer from them geophysical properties about the Earth [29]. For the cryosphere, examples include using changes in the gravitational field to estimate changes in the mass of glaciers and ice sheets as is done with the GRACE satellite. Other examples include using radars and lidars to measure the time of flight of signals reflected off the ice surface and use that information to measure elevation and elevation changes on sea ice and ice sheets. Finally, scattered solar radiation can be used to acquire hyper-spectral images for surface characterization and for traditional mapping of surface features.

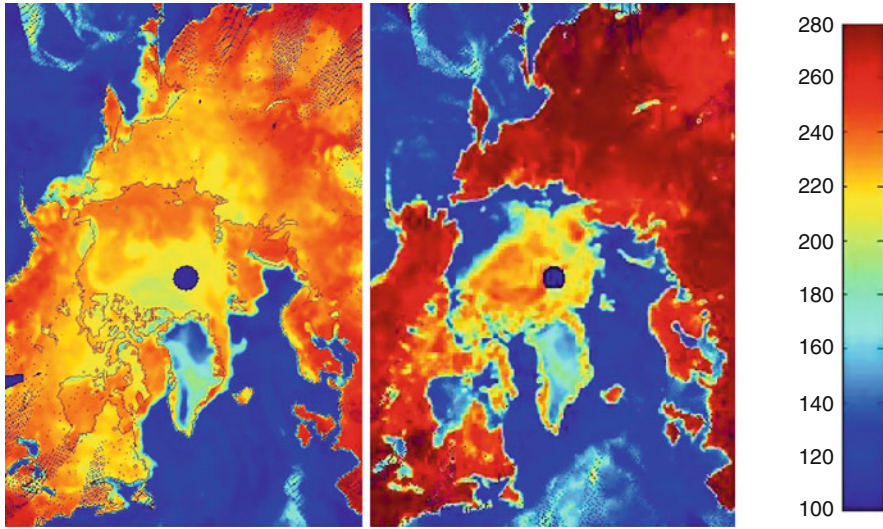


Fig. 2.5 19 GHz, horizontally polarized, special sensor microwave imager (SSM/I) brightness temperature data for the Arctic on February 15, 2004 (*left*) and August 25, 2004 (*right*). The brightness temperature scale (*far right*) is in degrees Kelvin. Differences between the emissivity of ocean, sea ice, land and ice sheets enable the relatively easy identification of the seasonal retreat in sea ice cover. Brightness temperature variations across the ice pack are caused by differences in ice type and age as well as in ice concentration

Accomplishing this task requires technical information about the behavior of the instrument, knowledge about the physical relationships between the measured field and the surface under study, and the development of algorithms that correctly invert the measured signal into some desired property [30, 31]. In some cases this task can be relatively easy. Because glacier ice is nearly homogeneous and because it is almost transparent at radar frequencies from about 1 to 500 MHz [32], the propagation time of a radar echo through the ice sheet and back can be converted to ice thickness by simply knowing the average ice dielectric constant, which in turn is readily convertible into a propagation velocity. In other cases, the task is more challenging because of heterogeneities in the material. The physical and electrical properties of sea ice change substantially as the ice ages [33]. This leads to changes in the thermally driven, microwave emission from the surface. The amount of energy received, measured in terms of a brightness temperature, is related to the product of the physical temperature and the emissivity of the surface. For open water, the microwave brightness temperature is cool because little energy escapes from the ocean surface. For sea ice, the brightness temperature is warm because more energy is transmitted across the electrically less reflective snow surface at these frequencies. Consequently, brightness temperature can be used to measure sea ice concentration and extent with high accuracy (several percent). Figure 2.5 shows that just on the basis of brightness temperature maps alone it is easy to distinguish the annual cycle of sea ice growth and decay across the arctic.

Sea Ice Extent, Concentration, Motion, and Thickness

Sea ice modulates polar climate by restricting the flow of heat from the relatively warm polar ocean into the relatively cold polar atmosphere. Because freezing ice preferentially rejects impurities from the crystalline lattice, the growth of sea ice modulates ocean circulation by releasing dense, cold brine that sinks beneath the marginal ice zones and initiates oceanic convection. Sea ice represents a natural barrier to surface navigation and so changes in sea ice cover have important consequences for future development of the Arctic. While sea ice is usually distinguishable from open ocean at optical wavelengths, cloud cover and the long polar night dictate the use of all-weather, day/night passive microwave radiometers for monitoring sea ice extent and concentration. As noted above, these radiometers measure the radiant energy emitted from the surface that, on one hand, can help identify ice type and age but, on the other hand, leads to complexities in designing more sophisticated instruments capable of sorting out whether the observed changes are due to different ice types populating a scene or because of change in the fractions of sea ice and open water in the scene. Moreover, the dimensions of the area sampled on the surface are often quite large (Hollinger and others [34] quote a field of view of 37×28 km for the SSMI 37 GHz vertically polarized channel). Consequently, approaches for estimating the concentration within a single pixel are required. A simple algorithm relies on the fact that the total emitted energy or equivalently the brightness temperature must equal the brightness temperature of the components in the scene times their respective concentrations within the pixel [35]. The component brightness temperatures are selected by tie points (such as a tie point for the brightness temperature of open water or first-year sea ice) which allows for a solution. More sophisticated algorithms attempt to better characterize regions where ice concentrations are low and where the data may be contaminated by weather effects. The results of these analyses are detailed measurements of ice extent which document the dramatic decrease in Arctic sea ice cover (Fig. 2.6). Graphs such as these represent some of the most compelling and straightforward evidence for changing climate at high latitudes.

Images such as those in Fig. 2.5 can also be used to document the coarse motion of the sea ice by tracking common features in repeat images. Better results are obtained with increasing resolution ranging from the several kilometer resolution obtainable with AVHRR to the very fine resolutions (tens of meters or less) achievable with SAR. Combined with airborne (Airborne Topographic Mapper flown as part of IceBridge) and space-borne (ERS-1/2, ICESat, Cryosat-2) altimeter estimates of ice thickness, circulation driven changes in ice thickness about Antarctica [36] and the total ice flux across the Arctic and out into the marginal seas can be computed. Based on ICESat estimates of sea ice freeboard, Kwok and others [37] estimate a 0.6 m thinning in Arctic multiyear ice for the period from 2003 to 2008.

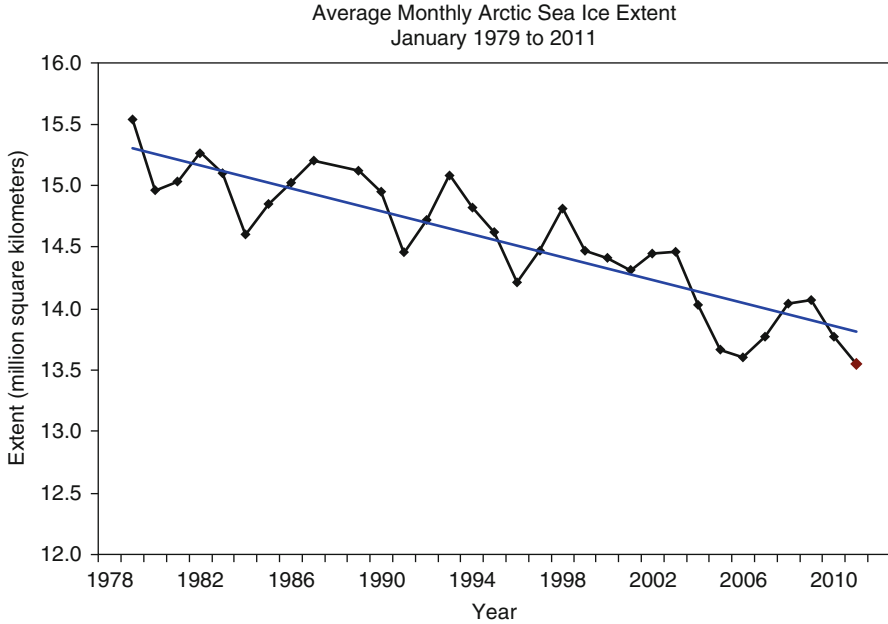


Fig. 2.6 Winter-time Arctic sea ice extent computed using passive microwave data. The decreasing trend illustrates the reduction in Arctic sea ice extent. There is a much more dramatic decline in ice extent during the summer months (Graph courtesy of the National Snow and Ice Data Center)

Regional Image Mapping of Glaciers and Ice Sheets

Airborne and space-borne image mapping of glaciers and ice sheets focuses on basic physical characteristics such as glacier termini, glacier snow lines, crevasse patterns, snow facies boundaries [38]. These properties have been successfully monitored with optical and microwave imaging instruments. As described in section “[Early History of Cryospheric Remote Sensing](#),” high latitude mapping began as early as 1962 with the launch of the Argon satellite. Shortly thereafter, the 1970s Landsat 1, 2, and 3 Multi-Spectral Scanner (MSS) images constitute an important glaciological resource [39, 40] and have been compiled into a series of beautiful folios edited by R. Williams Jr. and J. Ferrigno of the U.S. Geological Survey [see 41].

Compiling separate images into seamless, high-resolution digital maps of continental-scale areas is complicated by the data volume and the challenges in accurately estimating satellite orbits and instrument viewing geometries along orbit segments that might span from coast to coast. Initial successes in large-scale mapping were achieved through use of the moderate spatial resolution (1–2.5 km) and wide swath (2,400 km) Advanced Very High Resolution Radiometer (AVHRR) images [42] which helped reveal details about ice stream flow in West Antarctica [43]. After the original AVHRR mosaic of Antarctica, the United State Geological Survey (USGS) made subsequent improvements to the mosaic by eliminating more cloud, separating

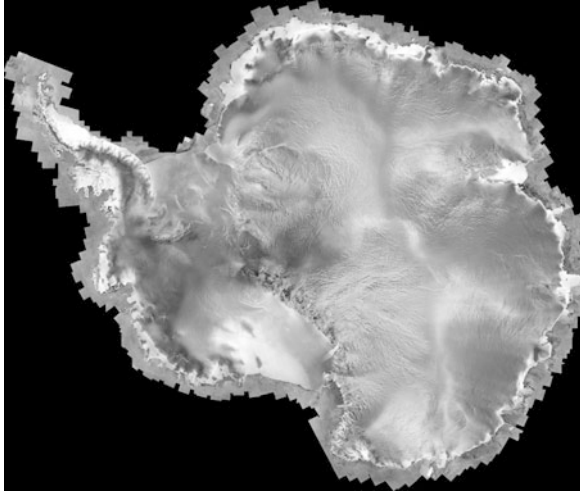


Fig. 2.7 Canadian RADARSAT-1 Antarctic Mapping Project synthetic aperture radar mosaic. The radar is sensitive to changes in the physical structure of the near surface snow. Bright coastal returns are scattered from subsurface ice lenses formed during fall freeze-up. Darker interior tones occur where snow accumulation is high. Other features such as ice streams and ice divides are visible (Map courtesy of K. Jezek. RADARSAT-1 data courtesy of the Canadian Space Agency)

the thermal band information to illustrate surface features more clearly, and correcting the coastline of the mosaic to include grounded ice while excluding thin, floating fast ice [44]. The European Earth Resources Satellite – 1 carried on board a synthetic aperture radar which allowed for large-scale regional mapping. Fahnestock and others [45] compiled a mosaic of Greenland which revealed the existence of a long ice stream in north east Greenland. In 1997, RADARSAT-1 synthetic aperture radar (SAR) data were successfully acquired over the entirety of Antarctica (Fig. 2.7). The coverage is complete and was used to create the first, high-resolution (25 m) radar image mosaic of Antarctica [46–48]. The image was used to map the ice sheet margin [49] and to investigate patterns of ice flow across Antarctica resulting in the discovery of large ice streams that drain from Coates Land into the Filchner Ice Shelf. Other large-scale mapping has been completed with MODIS for both the Arctic and the Antarctic [50]. Most recently, Landsat imagery of Antarctica has been compiled into a single, easily accessible map-quality data set [51] and SPOT stereo imagery has been used to derive digital elevation models of ice sheets, ice caps, and glaciers [52].

InSAR Measurements of Glaciers and Ice Sheets Surface Velocity

Glaciers and ice sheets move under the load of their own weight. They spread and thin in a fashion dictated by their thickness, the material properties of ice, and the

environmental conditions operative on the glacier surface, sides and bottom. The rate and direction of motion reveals important information about the forces acting on the glacier, provides knowledge about the rate at which ice is pouring into the coastal seas, and enables scientists to predict how the ice sheet might respond to changing global climate.

Since the International Geophysical Year of 1957–1958 and before, scientists have placed markers on the ice sheet and then, using a variety of navigation techniques from solar observations to GPS, have remeasured their positions to calculate motion. More recently, scientists have used high-resolution satellite images to track the position of crevasses carried along with the glacier to compute surface motion. These approaches are time consuming and result in patchy estimates of the surface velocity field. During the early 1990s, researchers at the Jet Propulsion Laboratory showed that synthetic aperture radar (SAR) offered a revolutionary new technique for estimating the surface motion of glaciers [53]. Here, the SAR is operated as an interferometer. That is, the distance from the SAR to a point on the surface is computed by measuring the relative number of radar-wave cycles needed to span the distance between the radar and the surface. Later, another measurement is made from a slightly different position and the numbers of cycles is computed again. The difference in the number of cycles combined with control points is used to estimate relative displacement to about one quarter of a radar-wave cycle (just a few centimeters for RADARSAT-1). Given an estimate of surface topography, this enables measurement of even the slowest moving portions of glaciers [54, 55]. A related approach relies on the fact that images formed from coherent radar signals scattered off a rough surface will have a small-scale-speckly appearance. The speckle pattern is random over scene but it is stable from scene to scene over a short time. Tracking the speckle pattern over time enables another measurement of surface velocity and while less accurate than the interferometric phase approach, speckle retracking has the advantage of yielding estimates of two components of the velocity vector [56, 57]. Typically a mixture of phase interferometry and speckle retracking are used in glacier motion studies.

Surface topography can also be estimated using InSAR techniques in cases where the surface velocities are small, the period between repeat observations is short [58], when multiple interferometric pairs are available [59], or when multiple antennas enable acquisition of interferometric data in a single pass as was done with NASA's Shuttle Radar Topographic Mission [60]. Although the surface elevation accuracy of InSAR topography is typically on the order of a few meters, the results can be used to estimate local slopes and also in comparison with earlier data provide a rough estimate of mass change.

Surface elevation and velocity data are key to studies of glacier dynamics [61]. InSAR data have been used to investigate the relative importance of different resistive stresses acting on ice streams and to predict the future behavior of ice streams and glaciers currently in retreat [62, 63]. Measurements on mostly retreating glaciers in the Himalayas [64], Patagonia [65, 66], European Alps [67], and Alaska (Fig. 2.8) document changing surface elevation and internal dynamics, and, together with estimates of ice thickness and surface accumulation rate, can provide a direct estimate of glacier mass loss [68].

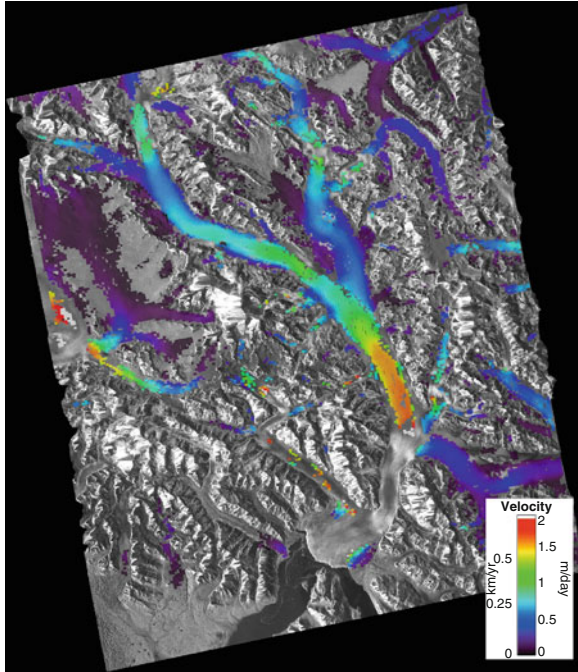


Fig. 2.8 Surface velocities on Hubbard Glacier Alaska measured using Japanese PALSAR L-band interferometric pairs. Hubbard Glacier is a tidewater glacier and ice from the advancing snout calves directly into Disenchantment Bay (*lower center*). Hubbard Glacier is one of the few in Alaska that is currently thickening and advancing (Image courtesy of E. W. Burgess and R. R. Forster, University of Utah)

Glaciers and Ice Sheets Mass Loss

Glaciers and ice sheets are reservoirs of freshwater with over 90% of Earth's freshwater bound in the Antarctic Ice Sheet [69], which when depleted have local, regional and global impacts. Indirect approaches for identifying whether ice sheets are losing mass include using proxy indicators such as surface melt area and duration – both measureable using passive microwave techniques [70, 71]. More directly, there are three primary remote sensing techniques currently used to assess the changing volume (or mass) of ice contained in glaciers [72]. The first involves an estimate of the difference between the annual net accumulation of mass on the surface of the glacier and the flux of ice lost from the terminus. The flux from the terminus is calculated using the measured ice thickness from airborne radar and the surface velocity, which is currently best estimated with InSAR [73]. The second approach is to measure surface elevation change. This has

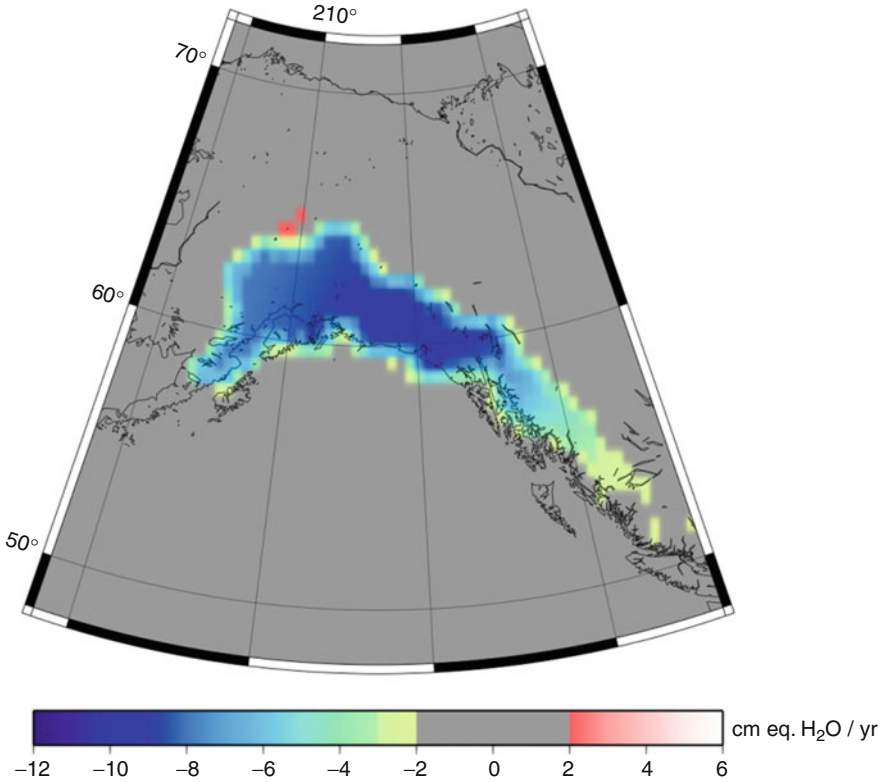


Fig. 2.9 Mass loss from Alaskan Glaciers in cm of water equivalent per year from GRACE (Image courtesy of S. Luthcke, NASA GSFC)

been accomplished with space-borne radar altimeters [74, 75] and airborne and space-borne lasers [76–78]. Finally, the changing glacial mass can be estimated directly by measuring changes in the gravity field as has been done with GRACE [79–81]. Figure 2.9 illustrates the estimated mass loss rate from Alaskan Glaciers as illustrated using GRACE data (Updated from [82]).

Recent analyses suggest these different techniques are yielding similar mass reductions for the Greenland Ice sheet [8, 83]. Thinning is primarily in the coastal regions where the rate of thinning has been increasing since the early 1990s and the current rates of mass loss estimated between 150 and 250 Gt/year. West Antarctica data indicate mass loss similar to Greenland, whereas East Antarctica retains a slightly positive (50 Gt/year) mass balance. Using surface mass balance estimates and GRACE gravity data, Rignot and others [84] report a combined ice sheet thinning rate of 475 ± 158 Gt/year. Cazenave and Llovel [8] conclude that for the period between 1993 and 2007 about 55% of total sea level rise can be attributed to melting of glaciers and ice sheets.

Fig. 2.10 Snow cover extent from NASA's MODIS.

Increasing shades of *gray* indicate greater percentages of snow cover within each pixel. *Brown* denotes snow-free surface



The Seasonal Snow Pack

Seasonal snow cover plays an important role in regional hydrology and water resource management. Rapid melting of the seasonal snow pack across the northern Great Plains in April 1997 resulted in catastrophic flooding of the Red River. From a climate perspective, the bright snow surface also serves as an effective mirror for returning incoming solar radiation back into space thus modulating the planetary heat budget.

The spectral reflectivity differences between snow, cloud, and other land cover types enables the seasonal snow cover to be routinely mapped globally using visible and infrared sensors such as NOAA's AVHRR, NASA's MODIS, and ESA's MERIS instruments. Snow may be mapped based on visual inspection of multi-spectral imagery. Automatic snow detection is accomplished by computing the normalized difference between, for example, the MODIS visible band (0.545–0.565 μm) and the near infrared band (1.628–1.652 μm). Snow is detected when the normalized difference exceeds a threshold value of 0.4 and when other criteria on land and cloud cover are met [85] (Fig. 2.10). Based on analysis of the NOAA 35 year data record, Dery and Brown [86] conclude that springtime snow extent across the northern hemisphere declined by some $1.28 \times 10^6 \text{ km}^2$ over a 35 year period.

Snow thickness and hence indirectly the mass of snow are key variables for estimating the volume of water available in a reservoir and potentially releasable as runoff. The most successful techniques to date have relied on passive-microwave-based algorithms. One approach for estimating snow thickness is to difference 19 and 37 GHz brightness temperature data that along with a proportionality constant yields an estimate of the snow thickness. The algorithm is based on the fact that 19 GHz radiation tends to minimize variations in ground temperature because it is less affected by the snow pack. The 37 GHz radiation is strongly scattered by the snow grains and brightness temperature at this frequency decreases rapidly with snow thickness/snow water equivalent. Factors which confuse this algorithm include topography and changes in ground cover [87].

Information about the seasonal onset of snowmelt can be obtained from microwave data. A few percent increase in the amount of free water in the snow pack causes the



Fig. 2.11 January 2010 NASA MODIS image of ice formed on the St. Lawrence River. Thin layers of new ice are distorted into swirls by the surface currents (*center left*). Thicker ice is held fast to the southern shore (Image courtesy of MODIS Rapid Response Team, NASA GSFC)

snow emissivity to approach unity resulting in a dramatic increase in passive microwave brightness temperature. This fact has been successfully used to track the annual melt extent on the ice sheets and also to track the springtime melt progression across the arctic. Higher resolution estimates of melt extent can be obtained with scatterometer and SAR data. These data generally show an earlier spring time date for the beginning of melt onset and a later date for the fall freeze [88].

Lake and River Ice

Lake and river ice form seasonally at mid and high latitudes and elevations. River ice forms under the flow of turbulent water which governs its thickness. The combination of ice jams on rivers with increased water flow during springtime snowmelt can result in catastrophic floods. Lake ice forms under less dynamic conditions resulting in a smoother ice surface that acts as an insulator to the underlying water. Hence lacustrine biology is strongly influenced by the formation of the ice canopy. The start of ice formation and the start of springtime ice break up are proxy indicators for changes in local climate as well as impacts on the ability to navigate these waterways.

Streams, rivers, lakes of all sizes dot the landscape. Locally, ice cover observations can be made from aircraft. Regionally or globally, river and lake ice monitoring is challenging because physical dimensions (long but narrow rivers) often require high resolution instruments like medium- to high-resolution optical data (Fig. 2.11) or SAR to resolve details [89]. Moreover, since the exact date of key processes, such as the onset of ice formation or river-ice breakup are unknown, voluminous data sets are required to support large-scale studies.

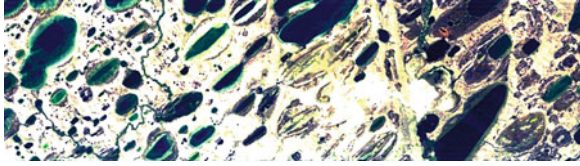


Fig. 2.12 EO-1 Hyperion satellite data acquired over the north coast of Alaska (70.5 N 156.5 W) and about 50 km inland from the coast, which is toward the *right* on this image. The image is 7.5 km wide (*top* to *bottom*). Color composite using channels 16 23 and 28

Permafrost

Permafrost presents one of the greatest challenges for regional remote sensing technologies [7, 90]. The near surface active layer, the shallow zone where seasonal temperature swings allow for annual freeze and thaw, is complicated by different soil types and vegetative cover. This combination tends to hide the underlying persistently frozen ground from the usual airborne and space-borne techniques mentioned above. Even in winter when the active layer is frozen, remote sensing of the permafrost at depth is extremely difficult because of the spatially variable electrical properties of the material. Thus far, the most successful airborne and space-borne remote sensing methods involve optical photography to identify surface morphologies as proxy indicators of the presence of permafrost. Patterned ground and pingos are examples of the types of features visible in optical imagery and that are diagnostic of underlying permafrost. SAR interferometry has been suggested as another tool that can be used to monitor terrain for slumping associated with thawing permafrost. Figure 2.12 shows E01 Hyperion satellite, visible-band data collected over the north slope of Alaska. Shallow, oval shaped lakes form in thermokarst, which develops when ice rich permafrost thaws and forms a hummocky terrain. Lakes and depressions left by drained lakes are densely distributed across the tundra. The long axis of the lake is oriented perpendicular to the prevailing wind direction. SAR intensity images have been used to determine that most of these small lakes freeze completely to the bottom during the winter months [91].

Recent Developments in Airborne Radar Ice Sounding of Glaciers

Today, airborne radars operating between about 5 and 500 MHz are the primary tools used for measuring ice sheet thickness, basal topography, and inferring basal properties over large areas. These radars are typically operated as altimeters and acquire profile data only along nadir tracks that are often separated by 5 or more kilometers. The along track resolution is met by forming a synthetic aperture and the vertical resolution of the thickness is met by transmitting high bandwidth signal.

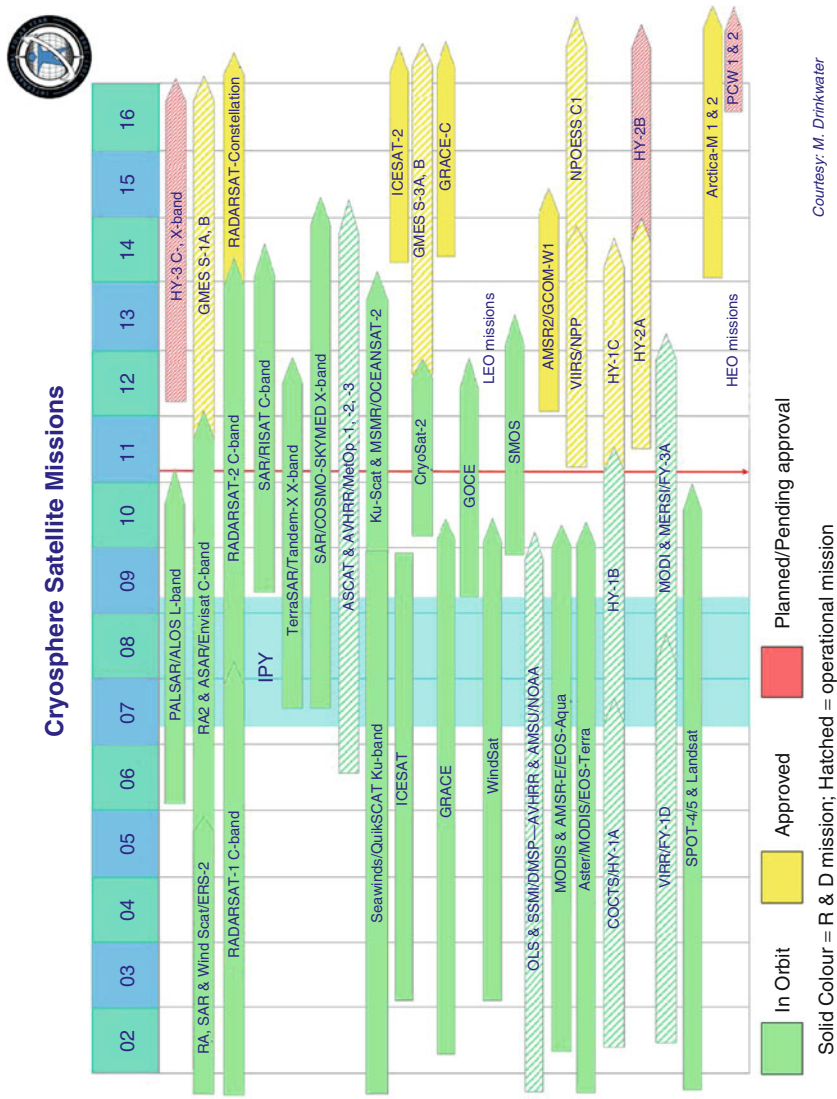
Even though highly accurate thickness measurements can be achieved, information in the third cross-track dimension is absent.

While the surface properties of the ice sheets are becoming increasingly well documented, the nature of the glacier bed remains obscured by its icy cover. Revealing basal properties, such as the topography and the presence or absence of subglacial water, is important if we are to better estimate the flux of ice from the interior ice sheet to the sea and to forecast anticipated changes of the size of the ice sheets. Recent experiments demonstrate how it is possible to go beyond airborne nadir sounding of glaciers and to produce three-dimensional images of the glacier bed. This development represents a major step forward in ice sheet glaciology by providing new information about the basal boundary conditions modulating the flow of the ice and revealing for the first time geomorphologic processes occurring at the bed of modern ice sheets. The approach relies on the application of radar tomography to UHF/VHF airborne radar data collected using multiple, independent antennas and receivers. Tomography utilizes phase and amplitude information from the independent receivers to isolate the direction of a natural target relative to the aircraft. Combined with the range to the target based on the echo travel time and position of the aircraft, tomographic methods yield swaths of reflectivity and topographic information on each side of the aircraft [92].

Cooperative Efforts to Observe, Monitor, and Understand the Cryosphere

Several cooperative, international scientific studies of the high latitudes have been organized. Beginning with the 1897 voyage of the *Belgica* to the Antarctic Peninsula and continuing to the 2007 International Polar Year, studies have relied on the most recent technologies to increase knowledge of the polar regions. To realize the benefit of the growing constellation of international satellites to the scientific objectives of the 2007 International Polar Year (IPY) (Fig. 2.13), the Global Interagency IPY Polar Snapshot Year (GIIPSY) project engaged the science community to develop consensus polar science requirements and objectives that could best and perhaps only be met using the international constellation of earth observing satellites [93]. Requirements focused on all aspects of the cryosphere and range from sea ice to permafrost to snow cover and ice sheets. Individual topics include development of high-resolution digital elevation models of outlet glaciers using stereo optical systems, measurements of ice surface velocity using interferometric synthetic aperture radar, and frequently repeated measurements of sea ice motion using medium resolution optical and microwave imaging instruments.

The IPY Space Task Group (STG), convened by the World Meteorological Organization (WMO), formed the functional link between the GIIPSY science community and the international space agencies. STG membership included representatives from the national space agencies of Italy, Germany, France, UK,



Courtesy: M. Drinkwater

Fig. 2.13 Current, approved and planned satellites for studying and monitoring the Cryosphere (Figure courtesy of Mark Drinkwater, European Space Agency)

US, Canada, Russia, China, Japan, and the European Space Agency (ESA), which in itself represents 19 nations. The STG determined how best to satisfy GIIPSY science requirements in a fashion that distributed the acquisition burden across the space agencies and recognized the operational mandates that guide the activities of each agency.

The STG adopted four primary data acquisition objectives for its contribution to the IPY. These are:

- Pole to coast multi-frequency InSAR measurements of ice-sheet surface velocity
- Repeat fine-resolution SAR mapping of the entire Southern Ocean sea ice cover for sea ice motion
- One complete high resolution visible and thermal IR (Vis/IR) snapshot of circumpolar permafrost
- Pan-Arctic high and moderate resolution Vis/IR snapshots of freshwater (lake and river) freeze-up and breakup

The STG achieved most of these objectives including: acquiring Japanese, ALOS L-band, ESA Envisat and Canadian Radarsat C-band, and German TerraSAR-X (Fig. 2.14) and Italian COSMO_SKYMED X band SAR imagery over the polar ice sheets [94]; acquiring pole to coast InSAR data for ice sheet surface velocity; optically derived, high-resolution digital elevation models of the perimeter regions of ice caps and ice sheets; coordinated campaigns to fill gaps in Arctic and Antarctic sea ice cover; extensive acquisitions of optical imagery of permafrost terrain; observations of atmospheric chemistry using the Sciamachy instrument.

Future Directions

Emerging sensor and platform technologies hold great promise for future airborne and space-borne remote sensing of the cryosphere. Airborne programs are likely to continue to use large manned aircraft in a fashion similar to NASA's IceBridge program which integrates a sophisticated suite of instruments including lidars, radars, gravimeters, magnetometers, optical mapping systems, and GPS. But there will also be a steady shift toward smaller, more dedicated unmanned aerial vehicles capable of remaining on station for longer periods and fulfilling some of the temporal coverage requirements that are difficult to satisfy with larger aircraft requiring a substantial number of crewmen.

It is worth noting again that ice sounding radars are exclusively deployed on aircraft for terrestrial research. This is driven operationally by the challenges of ionospheric distortions and by governmental controls on frequency allocations available for remote sensing applications designed to limit interference with communications and other commercial uses of the frequency bands. Certainly the latter is not an issue for other planetary studies and in fact the Martian ice caps have been successfully sounded from the orbiting MARSIS and SHARAD radars [95].

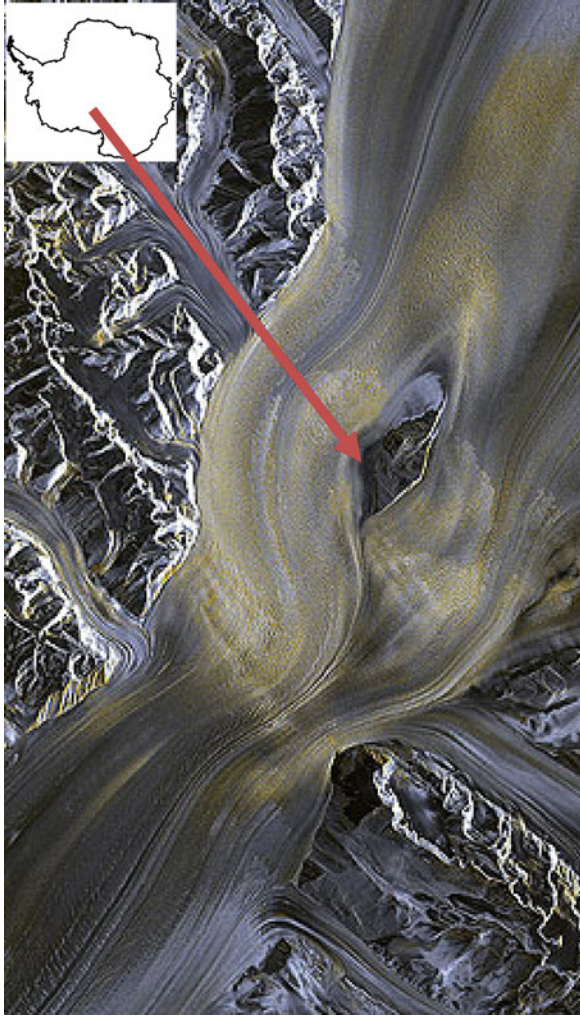


Fig. 2.14 German Aerospace Center TerraSAR-X observations of the Nimrod Glacier (inset map of Antarctica). Ice floes around a central nunatak and down toward the Ross Ice Shelf. Crevasses appear in conjunction with the interruption of flow by the nunatak. Cooperative use of Canadian, German, European Space Agency, Italian, and Japanese synthetic aperture radar (SAR) satellites along with ground segment and data processing capabilities provided by the United States yielded a rich and diverse SAR data set that will be a lasting legacy of the IPY (TerraSAR-X data courtesy of D. Floricioiu, German Aerospace Center. Inset coastline derived from RADARSAT-1 Antarctic Mapping Project map)

These extraterrestrial successes motivate continuing interest in deploying similar instrument for observing Earth's ice cover in the future.

As indicated in [Fig. 2.13](#), there will be an ongoing constellation of satellites capable of collecting valuable cryospheric data. Here, coordination amongst the

different space faring nations will be key to realizing the greatest scientific benefit. Lessons about cooperation gleaned from the IPY can be profitably extended to the acquisition of data and the development of geophysical products beyond the polar regions to all sectors of the cryosphere. There could also be generally better integration of the atmospheric chemistry and polar meteorological communities, as well as incorporation of gravity and magnetic geopotential missions into the coordination discussions. It is also possible to envision discussion and collaboration on emerging technologies and capabilities such as the Russian Arktika Project [96] and advanced subsurface imaging radars. A primary objective of continued coordination of international efforts is securing collections of space-borne “snapshots” of the cryosphere through the further development of a virtual Polar Satellite Constellation [97]. A natural vehicle for adopting lessons learned from GIIPSY/STG into a more encompassing international effort could be the Global Cryosphere Watch [98] recently proposed by WMO to be in support of the cryospheric science goals specified for the Integrated Global Observing Strategy Cryosphere Theme [1].

Bibliography

Primary Literature

1. IGOS (2007) Integrated global observing strategy cryosphere theme report – for the monitoring of our environment from space and from Earth. WMO/TD-No. 1405. World Meteorological Organization, Geneva, 100p
2. Perovich D, Light B, Eicken H, Jones K, Runciman K, Nghiem S (2007) Increasing solar heating of the Arctic ocean and adjacent seas, 1979–2005: attribution and role in the ice-albedo feedback. *Geophys Res Lett* 34:L19505. doi:[10.1029/2007GL031480](https://doi.org/10.1029/2007GL031480)
3. Perovich D, Richter-Menge J, Jones K, Light B (2008) Sunlight, water and ice: extreme arctic sea ice melt during the summer of 2007. *Geophys Res Lett* 35:L11501. doi:[1029/2008GL034007](https://doi.org/10.1029/2008GL034007)
4. Ainley D, Tynan C, Stirling I (2003) Sea ice: a critical habitat for polar marine mammals. In: Thomas D, Dieckmann G (eds) *Sea ice: an introduction to its physics, chemistry, biology and geology*. Blackwell Science, Oxford, pp 240–266
5. Arrigo K (2003) Primary production in sea ice. In: Thomas D, Dieckmann G (eds) *Sea ice: an introduction to its physics, chemistry, biology and geology*. Blackwell Science, Oxford, pp 143–183
6. Lizotte M (2003) The microbiology of sea ice. In: Thomas D, Dieckmann G (eds) *Sea ice: an introduction to its physics, chemistry, biology and geology*. Blackwell Science, Oxford, pp 184–210
7. Grosse G, Romanovsky V, Jorgenson T, Water Anthony K, Brown J, Overduin P (2011) Vulnerability and feedbacks of permafrost to climate change. *EOS* 92(9):73–74
8. Cazenave A, Llovel W (2010) Contemporary sea level rise. *Ann Rev Mar Sci* 2:145–173
9. Prowse TD, Bonsal B, Duguay C, Hessen D, Vuglinsky V (2007) River and lake ice. In: Eamer J, Ahlenius H, Prestrud P, United Nations Environment Programme et al (eds) *Global outlook for ice and snow*. United Nations Environment Programme, Nairobi, pp 201–214. ISBN 978-92-807-2799-9

10. Kim Y, Kimball J, McDonald K, Glassy J (2011) Developing a global data record of daily landscape freeze/thaw status using satellite passive microwave remote sensing. *IEEE Trans Geosci Remote Sens* 49(3):949–960
11. McKinley AC (1929) *Applied aerial photography*. Wiley, New York, 341p
12. Mittelholzer W and others (1925) *By airplane towards the north pole* (trans: Paul E, Paul C). Houghton Mifflin, Boston, 176p
13. Wilkins H (1929) The Wilkins-Hearst Antarctic Expedition, 1928–1929. *Geogr Rev* 19(3):353–376
14. Wilkins H (1930) Further Antarctic explorations. *Geogr Rev* 20(3):357–388
15. Byrd RE (1930) *Little America*. G.P. Putman's Sons, New York, 422p
16. McDonald RA (1995) Corona: success for space reconnaissance, a look into the cold war and a revolution in intelligence. *Photogramm Eng Remote Sens* 61(6):689–720
17. Peebles C (1997) *The Corona Project: America's First Spy Satellites*. Naval Institute Press, Annapolis, 351p
18. Wheelon AD (1997) Corona: the first reconnaissance satellites. *Phys Today* 50(2):24–30
19. Richelson JT (1998) Scientists in black. *Sci Am* 278(2):48–55
20. Sohn HS, Jezek KC, van der Veen CJ (1998) Jakobshavn Glacier, West Greenland: 30 years of spaceborne observations. *Geophys Res Lett* 25(14):2699–2702
21. Zhou G, Jezek KC (2002) 1960s era satellite photograph mosaics of Greenland. *Int J Remote Sens* 23(6):1143–1160
22. Bindshadler RA, Vornberger P (1998) Changes in the West Antarctic ice sheet since 1963 from declassified satellite photography. *Science* 279:689–692
23. Kim K, Jezek KC, Sohn H (2001) Ice shelf advance and retreat rates along the coast of Queen Maud Land, Antarctica. *J Geophys Res* 106(C4):7097–7106
24. Kim K, Jezek K, Liu H (2007) Orthorectified image mosaic of the Antarctic coast compiled from 1963 Argon satellite photography. *Int J Remote Sens* 28(23–24):5357–5373
25. Waite AH, Schmidt SJ (1962) Gross errors in height indication from pulsed radar altimeters operating over thick ice or snow. *Proc IRE* 50(6):1515–1520
26. Bogorodsky VV, Bentley CR, Gudmandsen PE (1985) *Radioglaciology*. D. Reidel, Dordrecht, 254p
27. Fisher E, McMechan G, Gorman M, Cooper A, Aiken C, Ander M, Zumbege M (1989) Determination of bedrock topography beneath the Greenland ice sheet by three-dimensional imaging of radar sounding data. *J Geophys Res* 94(B3):2874–2882
28. Koenig L, Martin S, Studinger M (2010) Polar airborne observations fill gap in satellite data. *EOS* 91(38):333–334
29. Schanda E (1986) *Physical fundamentals of remote sensing*. Springer, Berlin, 187p
30. Hall D, Martinec J (1985) *Remote sensing of ice and snow*. Chapman and Hall, New York, 189p
31. Rees WG (2006) *Remote sensing of snow and ice*. Taylor and Francis Group, Boca Raton, 285p
32. Petrenko VF, Whitworth RW (1999) *Physics of ice*. Oxford University Press, Oxford, 373p
33. Carsey FD (ed) (1992) *Microwave remote sensing of sea ice*, A.G.U. geophysical monograph 68. American Geophysical Union, Washington, DC, 462p
34. Hollinger J, Peirce J, Poe G (1990) SSM/I instrument evaluation. *IEEE Trans Geosci Remote Sens* 28(5):781–790
35. Parkinson C, Gloersen P (1993) Global sea ice cover. In: Gurney R, Foster J, Parkinson C (eds) *Atlas of satellite observations related to global change*. Cambridge University Press, Cambridge, pp 371–383
36. Zwally HJ, Yi D, Kwok R, Zhao Y (2008) ICESat measurements of sea ice freeboard and estimates of sea ice thickness in the Weddell sea. *J Geophys Res* 113:C02S15. doi:[10.1029/2007JC004284](https://doi.org/10.1029/2007JC004284)
37. Kwok R, Cunningham G, Wensnahan M, Rigor I, Zwally HJ, Yi D (2009) Thinning and volume loss of the Arctic ocean sea ice cover:2003–2008. *J Geophys Res* 114:C07005. doi:[10.1029/2009JC005312](https://doi.org/10.1029/2009JC005312)

38. Williams R Jr, Hall D (1993) Glaciers. In: Gurney R, Foster J, Parkinson C (eds) Atlas of satellite observations related to global change. Cambridge University Press, Cambridge, pp 401–422
39. Swithinbank C (1973) Higher resolution satellite pictures. *Polar Rec* 16(104):739–751
40. Swithinbank C, Lucchitta BK (1986) Multispectral digital image mapping of Antarctic ice features. *Ann Glaciol* 8:159–163
41. U.S. Geological Survey (2010) Satellite image atlas of glaciers of the world. USGS Fact Sheet FS 2005-3056, 2p
42. Merson RH (1989) An AVHRR mosaic of Antarctica. *Int J Remote Sens* 10:669–674
43. Bindschadler R, Vornberger P (1990) AVHRR imagery reveals Antarctic ice dynamics. *EOS* 71:741–742
44. Ferrigno JG, Mullins JL, Stapleton JA, Chavez PS Jr, Velasco MG, Williams RS Jr (1996) Satellite image map of Antarctica, Miscellaneous investigations map series 1-2560. U.S Geological Survey, Reston
45. Fahnestock MR, Bindschadler RK, Jezek KC (1993) Greenland ice sheet surface properties and ice dynamics from ERS-1 SAR imagery. *Science* 262:1525–1530
46. Jezek KC (2008) The RADARSAT-1 Antarctic Mapping Project. BPRC Report No. 22. Byrd Polar Research Center, The Ohio State University, Columbus, 64p
47. Jezek KC (1999) Glaciologic properties of the Antarctic ice sheet from spaceborne synthetic aperture radar observations. *Ann Glaciol* 29:286–290
48. Jezek K (2003) Observing the Antarctic ice sheet using the RADARSAT-1 synthetic aperture radar. *Polar Geogr* 27(3):197–209
49. Liu H, Jezek K (2004) A complete high-resolution coastline of Antarctica extracted from orthorectified Radarsat SAR imagery. *Photogramm Eng Remote Sens* 70(5):605–616
50. Scambos TA, Haran T, Fahnestock M, Painter T, Bohlander J (2007) MODIS-based mosaic of Antarctica (MOA) data sets: continent-wide surface morphology and snow grain size. *Remote Sens Environ* 111(2–3):242–257
51. Bindschadler R, Vornberger P, Fleming A, Fox A, Mullins J, Binnie D, Paulsen S, Granneman B, Gorodetzky D (2008) The Landsat image mosaic of Antarctica. *Remote Sens Environ* 112(12):4214–4226
52. Korona J, Berthier E, Bernarda M, Rémy F, Thouvenot E (2008) SPIRIT. SPOT 5 stereoscopic survey of Polar Ice: reference images and topographies during the fourth International Polar Year (2007–2009). *ISPRS J Photogramm Remote Sens* 64(2):204–212. doi:[10.1016/j.isprsjprs.2008.10.005](https://doi.org/10.1016/j.isprsjprs.2008.10.005)
53. Goldstein RM, Englehardt H, Kamb B, Frohlich R (1993) Satellite radar interferometry for monitoring ice sheet motion: application to an Antarctic ice stream. *Science* 262:1525–1530
54. Kwok R, Fahnestock M (1996) Ice sheet motion and topography from radar interferometry. *IEEE Trans Geosci Remote Sens* 34(1):189–199
55. Joughin I, Kwok R, Fahnestock M (1996) Estimation of ice-sheet motion using satellite radar interferometry: method and error analysis with application to Humboldt Glacier, Greenland. *J Glaciol* 42(142):564–575
56. Gray AL, Short N, Matter KE, Jezek KC (2001) Velocities and ice flux of the Filchner Ice Shelf and its tributaries determined from speckle tracking interferometry. *Can J Remote Sens* 27(3):193–206
57. Joughin I (2002) Ice-sheet velocity mapping: a combined interferometric and speckle-tracking approach. *Ann Glaciol* 34(1):195–201
58. Eldhuset P, Andersen S, Hauge EI, Weydahl D (2003) ERS tandem InSAR processing for DEM generation, glacier motion estimation and coherence analysis on Svalbard. *Int J Remote Sens* 24(7):1415–1437
59. Rignot E, Forster R, Isaacs B (1996) Mapping of glacial motion and surface topography of Hielo Patagónico Norte, Chile, using satellite SAR L-band interferometry data. *Ann Glaciol* 23:209–216

60. Surazakov A, Aizen V (2006) Estimating volume change of mountain glaciers using SRTM and map-based topographic data. *IEEE Trans Geosc Remote Sens* 44(10): 2991–2995
61. Joughin I, Gray L, Bindschadler R, Price S, Morse D, Hulba C, Mattar K, Werner C (1999) Tributaries of West Antarctic ice streams revealed by RADARSAT interferometer. *Science* 286:283–286
62. Stearns L, Jezek K, Van der Veen CJ (2005) Decadal scale variations in ice flow along Whillans ice stream and its tributaries, West Antarctica. *J Glaciol* 51(172): 147–157
63. Beem L, Jezek K, van der Veen CJ (2010) Basal melt rates beneath the Whillans ice stream, West Antarctica. *J Glaciol* 56(198):647–654
64. Luckman L, Quencyand D, Beven S (2007) The potential of satellite radar interferometry and feature tracking for monitoring flow rates of Himalayan glaciers. *Remote Sens Environ* 111:172–181
65. Floricioiu D, Eineder M, Rott H, Yague-Martinez N, Nagler T (2009) Surface velocity and variations of outlet glaciers of the Patagonia Icefields by means of TerraSAR-X. In: *Geoscience and remote sensing symposium, IGARSS 2009*, vol 2, Cape Town, 12–17 Jul 2009, pp 1028–1031
66. Forster R, Rignot E, Isacks B, Jezek K (1999) Interferometric radar observations of the Hielo Patagonico Sur, Chile. *J Glaciol* 45(150):325–337
67. Paul F, Haeberli W (2008) Spatial variability of glacier elevation changes in the Swiss Alps obtained from two digital elevation models. *Geophys Res Lett* 35:L21502. doi:[10.1029/2008GL034718](https://doi.org/10.1029/2008GL034718)
68. Yu J, Liu H, Jezek K, Warner R, Wen J (2010) Analysis of velocity field, mass balance, and basal melt of the Lambert Glacier system by incorporating Radarsat SAR interferometry and ICESat laser altimeter measurements. *J Geophys Res* 115:B11102. doi:[10.1029/2010JB007456](https://doi.org/10.1029/2010JB007456)
69. Thomas RH (1993) Ice sheets. In: Gurney R, Foster J, Parkinson C (eds) *Atlas of satellite observations related to global change*. Cambridge University Press, Cambridge, pp 385–400
70. Bhattacharya I, Jezek K, Wang L, Liu H (2009) Surface melt area variability of the Greenland ice sheet: 1979–2008. *Geophys Res Lett* 36:L20502. doi:[10.1029/2009GL039798](https://doi.org/10.1029/2009GL039798)
71. Liu H, Wang L, Jezek K (2006) Spatio-temporal variations of snow melt zones in Antarctic ice sheet derived from satellite SMMR and SSM/I data (1978–2004). *J Geophys Res* 111:F01003. doi:[10.1029/2005JF0000318](https://doi.org/10.1029/2005JF0000318)
72. Rignot E, Thomas R (2002) Mass balance of the polar ice sheets. *Science* 297(5586):1502–1506
73. Rignot E, Kanagaratnam P (2006) Changes in the velocity structure of the Greenland ice sheet. *Science* 311(5673):986–990
74. Zwally HJ, Giovinetto M, Li J, Cornejo H, Beckley M, Brenner A, Saba J, Yi D (2005) Mass changes of the Greenland and Antarctic ice sheets and shelves and contributions to sea-level rise: 1992–2002. *J Glaciol* 51(175):509–527
75. Wingham DJ, Shepherd A, Muir A, Marshall G (2006) Mass balance of the Antarctic ice sheet. *Philos Trans R Soc A* 364:1627–1635
76. Larsen CF, Motyka RJ, Arendt AA, Echelmeyer KA, Geissler PE (2007) Glacier changes in southeast Alaska and northwest British Columbia and contribution to sea level rise. *J Geophys Res Earth* 112:F01007
77. Thomas R, Frederick E, Krabill W, Manizade S, Martin C (2006) Progressive increase in ice loss from Greenland. *Geophys Res Lett* 33:L10503. doi:[10.1029/2006GL026075](https://doi.org/10.1029/2006GL026075)
78. Herzfeld UC, McBride PJ, Zwally HJ, Dimarzio J (2008) Elevation change in Pine Island Glacier, Walgreen Coast Antarctica, based on GLAS (2003) and ERS-1(1995) altimeter data analyses and glaciological implications. *Int J Remote Sens* 29(19):5533–5553. doi:[10.1080/01431160802020510](https://doi.org/10.1080/01431160802020510)

79. Chen J, Wilson C, Blankenship D, Tapley B (2009) Accelerated Antarctic ice loss from satellite gravity measurements. *Nat Geosci* 2. doi:[10.1038/NCEO694](https://doi.org/10.1038/NCEO694)
80. Luthcke SB, Zwally HJ, Abdalati W, Rowlands D, Ray R, Nerem R, Lemoine F, McCarthy J, Chinn D (2006) Recent Greenland ice mass loss by drainage system from satellite gravity observations. *Science* 314(5803):1286–1289
81. Velicogna I (2009) Increasing rates of ice mass loss from the Greenland and Antarctic ice sheets revealed by GRACE. *Geophys Res Lett* 36:L19503. doi:[10.1029/2009GL040222](https://doi.org/10.1029/2009GL040222)
82. Luthcke S, Arendt A, Rowlands D, McCarthy J, Larsen C (2008) Recent glacier mass changes in the Gulf of Alaska region from GRACE mascon solutions. *J Glaciol* 54(188):767–777
83. Thomas R, Davis C, Frederick E, Krabill W, Li Y, Manizade S, Martin C (2008) A comparison of Greenland ice-sheet volume changes derived from altimetry measurements. *J Glaciol* 54(185):203–212
84. Rignot E, Velicogna I, van den Broeke MR, Monaghan A, Lenaerts J (2011) Acceleration of the contribution of the Greenland and Antarctic ice sheets to sea level rise. *Geophys Res Lett* 38:L05503. doi:[10.1029/2011GL046583](https://doi.org/10.1029/2011GL046583)
85. Hall D, Riggs G, Salomonson V, DiGirolamo N, Bayr K (2002) MODIS snow-cover products. *Remote Sens Environ* 83:181–194
86. Dery S, Brown R (2007) Recent northern hemisphere snow cover extent trends and implications for the snow-albedo feedback. *Geophys Res Lett* 34:L22504. doi:[10.1029/2007GL031474](https://doi.org/10.1029/2007GL031474)
87. Foster J, Chang A (1993) Snow cover. In: Gurney R, Foster J, Parkinson C (eds) *Atlas of satellite observations related to global change*. Cambridge University Press, Cambridge, pp 361–370
88. Forster R, Long D, Jezek K, Drobot S, Anderson M (2001) The onset of Arctic sea-ice snow melt as detected with passive and active microwave remote sensing. *Ann Glaciol* 33:85–93
89. Jeffries M, Morris K, Kozlenko N (2005) Ice characteristics and processes, and remote sensing of frozen rivers and lakes. In: Duguay C, Piertroni A (eds) *Remote sensing of northern hydrology*, Geophysical monograph series 163. American Geophysical Union, Washington, DC, pp 63–90
90. Duguay C, Zhang T, Leverington D, Romanovsky V (2005) Satellite remote sensing of permafrost and seasonally frozen ground. In: Duguay C, Piertroni A (eds) *Remote sensing of northern hydrology*, Geophysical monograph series 163. American Geophysical Union, Washington, DC, pp 91–142
91. Jeffries M, Morris K, Liston G (1996) Method to determine lake depth and water availability on the north slope of Alaska with spaceborne imaging radar and numerical ice growth modeling. *Arctic* 49(4):367–374
92. Jezek K, Wu X, Gogineni P, Rodriguez E, Freeman A, Fernando-Morales F, Clark C (2011) Radar images of the bed of the Greenland ice sheet. *Geophys Res Lett* 38:L01501. doi:[10.1029/2010GL045519](https://doi.org/10.1029/2010GL045519)
93. Jezek K, Drinkwater M (2010) Satellite observations from the International Polar Year. *EOS Trans AGU* 91(14):125–126
94. Crevier Y, Rigby G, Werle D, Jezek K, Ball D (2010) A RADARSAT-2 snapshot of Antarctica during the 2007–08 IPY. *Newsl Can Antarct Res Netw* 28:1–5
95. Picardi G, Plaut JJ, Biccari D, Bombaci O, Calabrese D, Cartacci M, Cicchetti A, Clifford SM, Edenhofer P, Farrell WM, Federico C, Frigeri A, Gurnett DA, Hagfors T, Heggy E, Herique A, Huff RL, Ivanov AB, Johnson WTK, Jordan RL, Kirchner DL, Kofman W, Leuschen CJ, Nielsen E, Orosei R, Pettinelli E, Phillips RJ, Plettemeier D, Safaenili A, Seu R, Stofan ER, Vannaroni G, Watters TR, Zampolini E (2005) Radar soundings of subsurface Mars. *Science* 310(5756):1925–1928. doi:[10.1126/science.1122165](https://doi.org/10.1126/science.1122165)
96. Asmus VV, Dyaduchenko VN, Nosenko YI, Polishchuk GM, Selin VA (2007) A highly elliptical orbit space system for hydrometeorological monitoring of the Arctic region. *WMO Bull* 56(4):293–296

97. Drinkwater MR, Jezek KC, Key J (2008) Coordinated satellite observations during the International Polar Year: towards achieving a Polar Constellation. *Space Res Today* 171:6–17
98. Goodison B, Brown J, Jezek K, Key J, Prowse T, Snorrason A, Worby T (2007) State and fate of the polar cryosphere, including variability in the Arctic hydrologic cycle. *WMO Bull* 56(4): 284–292

Books and Reviews

- Gloersen P, Campbell W, Cavalieri D, Comiso J, Parkinson C, Zwally H (1992) Arctic and Antarctic sea ice, 1978–1987: satellite passive microwave observations and analysis, NASA SP-511. NASA, Washington, DC, 290p
- Parkinson C, Comiso J, Zwally H, Cavalieri D, Gloersen P, Campbell W (1987) Arctic sea ice, 1973–1976: satellite passive microwave observations, NASA SP-489. NASA, Washington, DC, 296p
- Schnack-Schiel S (2003) The macrobiology of sea ice. In: Thomas D, Dieckmann G (eds) *Sea ice: an introduction to its physics, chemistry, biology and geology*. Blackwell Science, Oxford, pp 211–239
- Weeks W, Hibler W (2010) *On sea ice*. University of Alaska Press, Fairbanks, 664p
- Zwally H, Comiso J, Parkinson C, Campbell W, Carsey F, Gloersen P (1983) Antarctic sea ice, 1973–1976: satellite passive microwave observations, NASA SP-459. NASA, Washington, DC, 206p

Earth System Monitoring
Selected Entries from the Encyclopedia of Sustainability
Science and Technology
Orcutt, J. (Ed.)
2013, VI, 518 p., Hardcover
ISBN: 978-1-4614-5683-4